# Hybrid Electric Aircraft with Unlike Engine Degradation Using Model Predictive Control

Halle E. Buescher
Intelligent Control and Autonomy Branch
NASA Glenn Research Center
Cleveland, Ohio 44135
Email: halle.e.buescher@nasa.gov

Elyse D. Hill
Dynamic Systems and Control Branch
NASA Langley Research Center
Hampton, Virginia 23666
Email: elyse.d.hill@nasa.gov

***Abstract*—The aviation industry is currently undertaking a revolution where either all-electric or hybrid-electric propulsion systems are becoming feasible and being considered for commercial transportation applications. The addition of electrical power systems to the propulsion system allows for the coupling of previously independently operated gas turbine engines. Commercial aircraft propulsion systems typically consist of multiple engines that may not degrade at the same rate. Asymmetric degradation on a multi-engine aircraft causes asymmetric thrust output from each engine. A hybrid-electric aircraft power and propulsion system architecture with electrified turbomachinery enables the power transfer between engines to balance asymmetric thrust. The concept, titled Hybrid-Electric Aircraft with Unlike Engine Degradation, utilizes a decentralized proportional-integral-based control approach to balance thrust production between the engines by transferring electrical power from a healthier to a more degraded engine. Building on this approach, this study presents a centralized model predictive controller (MPC) in lieu of the previous architecture to address constraint adherence and remove the need for multiple controllers. Simulation results are presented at varying engine degradation levels on a nonlinear hybrid-electric powertrain. Results show that the MPC successfully consolidates the previously decentralized control architecture into a single, centralized control scheme with the ability to balance thrust while subject to system constraints.**

***Keywords—control, hybrid-electric aircraft, electrified aircraft propulsion, sustainable flight, asymmetric thrust.***

## I. Introduction

In 2021, the U.S. Government published the Aviation Climate Action Plan, outlining a goal of net-zero carbon emissions in the aviation sector by 2050 [1]. NASA's Aeronautics Research Mission Directorate has made efforts towards this goal through projects such as the Electrified Powertrain Flight Demonstration and Advanced Air Transport Technology, which seek to develop and mature sustainable aviation technologies [2]. Electrification of powertrains is a sustainable alternative to fossil fuel-powered turbofan engines as electrification has the potential to reduce emissions in both the short and long-term of an aircraft's lifetime. Methods utilizing hybrid-electric propulsion systems that may lead to emissions reductions include Turbine Electrified Energy Management (TEEM), power extraction and insertion, and distributed electric propulsion [3, 4, 5]. TEEM exploits electric machines (EMs) coupled to the engine shafts to extract and insert power during engine transients for increased operability and performance [6]. Advancements have been made in control design by capitalizing on the increased number of control actuators resulting from the coupling of EMs with turbomachinery. These advanced designs have shown promising preliminary results, increasing compressor stability margins in a hardware-in-the-loop environment [7]. Though individual hybrid technologies may only provide a small benefit to the overall system, more significant benefits may be achieved when combining several technologies into one application.

Each engine on an aircraft may operate at varying levels of degradation, causing asymmetrical thrust distribution across the span of an airplane. Degraded engines burn hotter, their turbomachinery is less efficient, and they require more fuel to produce the same corrected fan speed, which is used as a proxy for thrust utilized by fuel flow rate control in the case of a turbofan [8]. As a result of these deficiencies, degradation produces more thrust. Asymmetric thrust distribution results in a yaw moment which is counteracted by a rudder trim adjustment to achieve the desired heading. However, increased trim of any control surface causes an increase in drag. With an increase in drag, the pilot or auto-throttle may compensate by increasing throttle, burning more fuel, and increasing thrust. Both the engine degradation and the drag present from control surface deflection cause an increase in fuel burn. If the more-degraded engine were able to compensate for its deficiencies with electrical power, rather than power from fuel, then the aircraft may balance the thrust asymmetry without increasing the fuel burn. By balancing the thrust asymmetry there is no longer a need to increase rudder trim. Without the need to increase rudder trim, drag and fuel burn remain constant.

The Hybrid Electric Aircraft with Unlike Engine Degradation (HEALED) control strategy was developed for hybrid-electric aircraft to compensate for thrust asymmetry [9]. This technique exploits the presence of an electrical power system with EMs coupled to the engine shafts to balance thrust asymmetry on an aircraft with multiple engines operating at different levels of degradation. Specifically, the method commands torque for power extraction or power insertion on the engine shafts to correct thrust asymmetry. Reference [9] implemented HEALED with proportional-integral (PI) controllers in a decentralized scheme. The methodology was shown to successfully balance asymmetric thrust and reduce fuel burn. While effective, this approach required multiple

controllers to accomplish the control goal, increasing control design complexity, and lacked more sophisticated considerations such as constraint adherence. To address these concerns, this study seeks to apply HEALED using model predictive control (MPC). Using a centralized MPC scheme, the proposed controller consolidates the control design into one framework that employs knowledge of the system model to command torques and adhere to system constraints. The proposed method is compared to the previous method and potential benefits are identified.

The remainder of the manuscript is organized as follows: Section II outlines the powertrain model of interest. Section III reviews the HEALED control strategy. Section IV details the proposed MPC controller, and results are presented and discussed in Section V. Finally, the paper is concluded in Section VI.

## II. Model Under Test

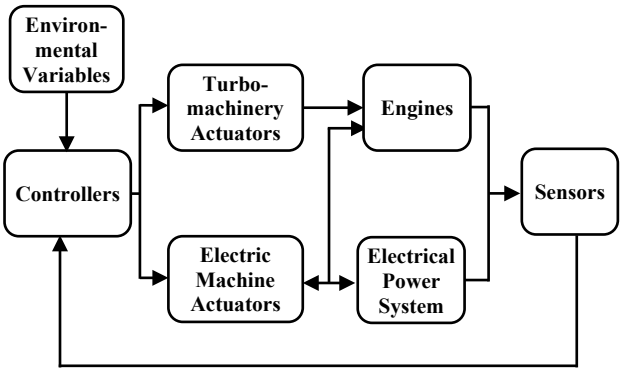


Fig. 1. High-Level Block Diagram of AGTF30 System; adapted from [10].

The dynamic system of interest is a two-engine aircraft propulsion system modeled using two 30,000 lbf thrust-class Advanced Geared Turbofan (AGTF30) engines with electrification [11]. Degradation is modeled using health parameters, or modification factors, applied to the fan, compressors, and turbines. A high-level block diagram of the electrified AGTF30 is shown in Fig. 1. Aircraft aerodynamic effects of rudder trim, yaw moment, drag estimate, and weight are not modeled. The nonlinear dynamics of the system are represented as a piecewise linear model for model-based control design purposes. The model was generated using an AGTF30 steady-state solver and linearization tool. [12]. Linearization occurs at specific operating points denoted by power lever angle (PLA), altitude (Alt), and Mach number (MN). The linear dynamic system, written in continuous time form with time argument $t$ omitted, is:

$$\delta\dot{x} = A\delta x + B\delta u \quad (1)$$

$$\delta y = C\delta x + D\delta u \quad (2)$$

where $x \in R^n$, $u \in R^m$, $y \in R^r$ are the state, input, and output vectors with respect to time, and $A, B, C, D$ are the state space matrices of the dynamic system. The $\delta$ notation indicates perturbations around steady-state operating conditions of the engine, denoted by the following relationships:

$$\delta x = x - x_{trim} \quad (3)$$

$$\delta u = u - u_{trim} \quad (4)$$

$$\delta y = y - y_{trim} \quad (5)$$

where the subscript $\cdot_{trim}$ represents the value of the input, state, or output vectors when the engine is at steady state. The states, inputs, and outputs of interest for this study are:

$$x = [N_{LPS} \quad N_{HPS}]^T \quad (6)$$

$$u = [W_f \quad M_{LPS} \quad M_{HPS}]^T \quad (7)$$

$$y = [N_{LPS} \;\; N_{HPS} \;\; T_{45} \;\; F_n \;\; SM_{Fan} \;\; SM_{LPC} \;\; SM_{HPC}]^T \quad (8)$$

Equation 6 denotes the speeds of the high- and low-pressure shafts (HPS, LPS), $N_{HPS}$ and $N_{LPS}$, respectively. Equation 7 denotes the fuel flow rate, $W_f$, and motor torques for the high- and low-pressure shafts, denoted $M_{HPS}$ and $M_{LPS}$, respectively. The outputs in (8) include the states, the low-pressure turbine temperature, $T_{45}$, engine net thrust, $F_n$, and the stall margins of the fan and of the high- and low-pressure compressors (HPC, LPC), denoted $SM_{Fan}$, $SM_{HPC}$, and $SM_{LPC}$, respectively. Note that while the stall margins cannot be directly measured, they can be calculated using measurable variables and empirical data and thus they are included in the output vector. Additionally, the input vector for the AGTF30 traditionally includes contributions from the open-loop scheduled variables of a variable area fan nozzle and a variable area bleed valve. For this study, those actuators were omitted from the state space, but can be included in future implementations.

The variables in (1) – (8) can be further subscripted with $\cdot_H$ or $\cdot_D$ to denote belonging to a less-degraded (healthier) or more-degraded engine, respectively. Further, the state space matrices associated with the more-degraded engine are representative of varying levels of engine degradation, either half-life or end-of-life, while those associated with the healthier engine are considered undegraded. The EMs of the more-degraded and healthier engines are related by the following equation:

$$[M_{LPS,D} \quad M_{HPS,D}]^T = -\eta[M_{LPS,H} \quad M_{HPS,H}]^T \quad (9)$$

where $\eta \leq 1$ is an efficiency ratio. The negative sign in (9) expresses the relationship between power extraction and power injection among the healthier and more-degraded engines. Because of this coupling, the motors on the healthier and more-degraded engines cannot be controlled independently of one another. This dependency is discussed in the following section. A conceptual diagram of the electrical power system considered in this study is shown below in Fig. 2.

## III. HEALED

The goal of HEALED is to balance thrust by exploiting a hybridized aircraft powertrain. The aircraft power and propulsion system is assumed to be hybridized with EMs coupled to both shafts of each engine. Thrust from each engine is assumed to be known. For simplicity, and with an intension to focus on control development, the electrical power system (EPS), shown in detail in Fig. 2, is modeled only by (9). Power extracted from the healthier engine, multiplied by the EPS efficiency ratio, is equal to power inserted on the degraded

engine. Shown in Fig. 2, the bus connecting the LPS EMs and the bus connecting the HPS EMs are separate. This prohibits power sharing between LPS and HPS shafts, which is something that can be explored in future work.

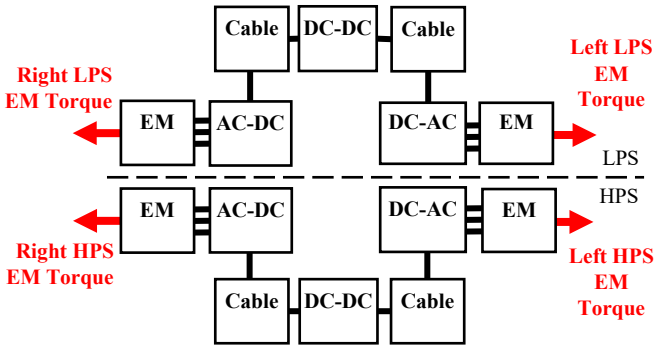


Fig. 2. Electrical power system utilized to demonstrate HEALED control; adapted from [9].

The previous HEALED methodology introduced in [9], termed HEALED PI, lacked the ability to account for system constraints and required intensive gain scheduling to accomplish thrust balancing. Implementing HEALED with MPC attempts to circumvent these pitfalls by exploiting the advantages of this optimal control method, which include system knowledge and constraint adherence. Both HEALED controllers are compared to a fuel flow rate controller with no consideration to thrust balancing (Baseline Control). While the controllers contain this baseline logic, they also include additional considerations for thrust balancing. A block diagram for both Baseline Control and HEALED is shown in Fig. 3. The following subsections give brief overviews for the baseline and HEALED PI control scenarios.

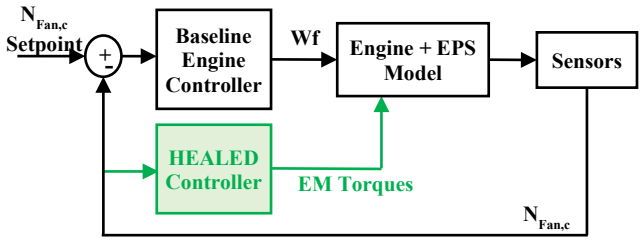


Fig. 3. Baseline control with HEALED for a hybrid-electric aircraft; augmentations to the baseline are shown in green.

### A. *Baseline Control*

Baseline Control uses corrected fan speed, $N_{Fan,c}$, as a thrust proxy and generates a fuel flow rate command, $W_f$, for each engine. In the AGTF30 system, fan speed is related to the LPS shaft speed by a gear ratio expressed by $N_{Fan} = N_{LPS}/3.1$. Corrected fan speed is determined using a lookup table that is a function of MN, PLA, and Alt. For this paper, a twin-engine aircraft with both engines receiving identical PLA inputs will be assumed, resulting in both engines operating at the same $N_{Fan,c}$. A more degraded engine will burn more fuel for the same $N_{Fan,c}$ when compared to a healthier engine. The result is an increase in thrust from the degraded engine.

### B. *HEALED PI*

HEALED control maintains the baseline control, using $N_{Fan,c}$ as a thrust proxy while generating a $W_f$ command for each engine. Assuming perfect thrust estimation, the difference in thrust determines a symmetry error, which is the primary input to HEALED control. In [9], the HEALED PI control block consists of one PI controller for each electric machine. To prevent power imbalance within the engine, this control commands EM torques for each shaft at a ratio proportional to the shaft speeds for insertion and extraction. HEALED PI is shown to balance thrust on a multi-engine aircraft with uneven degradation. By inserting power on the more-degraded engine shafts, the system compensates for the less efficient turbomachinery with electrical power rather than an increase in fuel burn. With power transfer, EMs are commanded to extract power from the healthier engine and insert power on the more-degraded engine. As a result, the healthier engine burns more fuel, generating more thrust, and the more-degraded engine burns less fuel, generating less thrust. After both thrusts balance out, and ensuring net thrust is consistent, the EMs hold their commanded extraction and insertion setpoints for steady state operation. Ideally, since the healthier engine is more efficient at generating thrust compared to the more-degraded engine, when power is extracted and the baseline control increases fuel burn to maintain fan speed, total fuel burn from both engines is reduced for the same thrust response. In other words, the reduction in fuel burn on the more-degraded engine is larger than the increase in fuel burn on the healthier engine leading to a net reduction.

Reference [9] compared HEALED PI to an alternative, non-hybrid-electric thrust balancing controller, the Engine Performance Deterioration Mitigating Controller, and the Baseline Control [13]. Both controllers successfully balance thrust in simulation. When compared to the other controller, HEALED PI reduced the amount of fuel burned on an already hybridized system.

## IV. HEALED WITH MODEL PREDICTIVE CONTROL

MPC is an optimal control technique that determines a control input over a prediction horizon with respect to system constraints [14]. Because of its ability to manage complex systems while balancing numerous system goals with minimal conceptual complexity, MPC has seen increased use in electrified aircraft propulsion applications in recent years [15, 16, 17, 18]. Indeed, its ability to adhere to constraints has made it a desirable architecture over more traditional control techniques, such as PI methods.

The primary control goal of the HEALED MPC is to reduce the difference between the more-degraded engine and healthier engine thrusts by leveraging EMs and an EPS. The optimal control problem for the proposed architecture is stated in discrete time as:

$$\min_{\delta u_k} J_k = \frac{1}{2}\sum_{j=1}^{N_p} ||\delta\tilde{y}_{k+j}||_Q^2 + \frac{1}{2}\sum_{j=0}^{N_u-1} ||\Delta u_{k+j}||_R^2 \quad (11)$$

subject to

$$\begin{aligned}
&\delta y_k = y_0 \\
&\delta x_{k+1} = A_d\delta x_k + B_d\delta\Omega_k \\
&\delta y_k = C_d\delta x_k + D_d\delta\Omega_k \\
&\delta x_k \in X - x_{trim} \\
&\delta u_k \in U_{2:3} - u_{trim,\ 2:3} \\
&\delta y_k \in Y - y_{trim} \\
&k \in 1, \ldots, N
\end{aligned}$$

where $k, j$ are index variables for time and horizon lengths, $N \geq N_u$ are the prediction and control horizons, $Q,R$ are the output and input weighting matrices, $X,\ U,$ and $Y$ are the state, input, and output constraint sets, and the representation $\|\cdot\|_\Pi^2$ denotes the weighted Euclidean norm where the weight $\Pi$ is a symmetric, positive-definite matrix. The subscript $\cdot_d$ indicates the discretized form of the state space matrix, and the subscript $\cdot_{2:3}$ indicates the second and third elements of (7). The variables $\tilde{y}$ and $\Delta u$ are:

$$\tilde{y} = F_{n,D} - F_{n,H} \quad (12)$$

$$\Delta u_{k+j} = \delta u_{k+j} - \delta u_{k+j-1} \quad (13)$$

where (12) represents an output tracking term between the healthier and degraded engine thrusts and (13) represents an input rate term. The variable $\Omega$ is an augmented input vector that allows the controller to account for non-optimized inputs:

$$\Omega_k = -[W_{f,H,\,0} \quad M_{LPS,H,k} \quad M_{HPS,H,k}]^T \quad (14)$$

where the fuel flow rate term is initialized at the current time instant and held constant over the horizon while the EM terms are optimized. This approach prevents potential information loss from having a reduced state space model and is viable at small sampling times and horizon lengths.

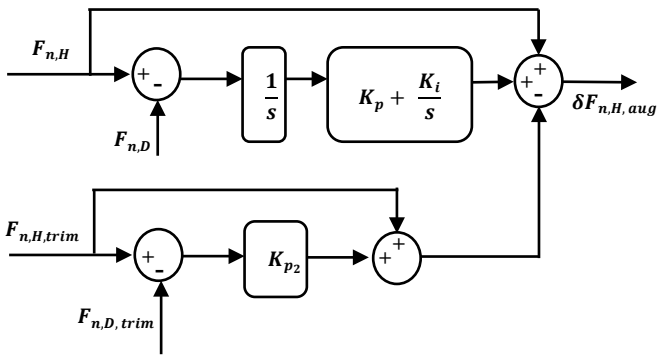


Fig. 4. Trajectory augmentation controller included with HEALED MPC.

Fig. 4 depicts a Trajectory Augmentation mechanism used to mitigate steady-state error during implementation of the controller. The augmentation is composed of a PI controller, responsible for augmenting the target $F_{n,H}$ based on the error between $F_{n,H}$ and $F_{n,D}$, and a proportional controller, responsible for augmenting the healthier engine trim, $F_{n,H,trim}$, based on the difference between $F_{n,H,trim}$ and $F_{n,D,\,trim}$. The result is an augmented target, $F_{n,H,aug}$, used in (12) in place of $F_{n,H}$. The latter controller was added to accommodate the difference in the thrust trim values for the healthier and more-degraded engines. If left unaccounted for, the difference in trims produces a constant steady-state error that the PI corrector alone cannot overcome. As the trims are constant at steady-state conditions, an integral term would not benefit the trim proportional controller. Currently, integrator windup is not accounted for in the trajectory augmentation mechanism but should be explored.

## V. Results

The proposed controller is verified on a tracking scenario at a cruise condition (Alt = 35 kft, MN = 0.8, standard day) for two different engine degradation scenarios: 50% degradation and 100% degradation. A 0% degradation scenario is also included to verify controller function. Only one engine is degraded for this simulation, and the other, the healthier engine, is set to 0% degradation. The proposed controller is compared to the Baseline Control and the HEALED PI. The HEALED MPC is implemented in MATLAB®/Simulink® using the Newton-Raphson root finding method. Input constraints are enforced via clipping and output constraints are enforced using a barrier function of the form:

$$g(x) = \frac{s}{x - x_{lb}} + \frac{s}{x_{ub} - x} - \frac{4}{x_{ub} - x_{lb}} \quad (15)$$

where $s$ is the sharpness of the barrier function, indicating its steepness at the bounds. The terms $x_{lb}$ and $x_{ub}$ represent a variable's lower and upper bounds, respectively. The sampling time is set to $T_s = 0.02$ sec while the prediction and control horizons are $N = 5$ and $N_u = 3$. The weight matrices for the MPC are $Q = 1$ and $R_0 = diag([5 \quad 5]^T)$. The value of $R$ is made time-varying during the simulation according to the equation $R = R_0 + I_m \frac{\nu}{(\hat{y})^2}$, where $\nu = 10$ and the notation $I_m$ indicates an identity matrix of size $m \times m$. Employing this equation permits the motors to produce torque quickly when the tracking error is large but to produce torque slowly when the tracking error is small. The trajectory augmentation gains are $K_i = 0.001$ and $K_p = 0.01$. The value for $K_{p,2}$ is 0.15 for 50% Degradation and 0.35 for 100% Degradation. The following constraint sets are used for the healthier engine system only:

$$X = \{0\ rpm \leq N_{LPS} \leq 7130\ rpm,\ 0\ rpm \leq N_{HPS} \leq 22500\ rpm\}$$

$$\begin{aligned}
Y = \{ &0\ rpm \leq N_{LPS} \leq 7130\ rpm,\ 0\ rpm \leq N_{HPS} \leq 22500\ rpm, \\
&2000\ °R \leq T_{45} \leq T_{45,\,max}\ °R,\ 8\% \leq SM_{Fan} \leq 80\%, \\
&8\% \leq SM_{LPC} \leq 40\%,\ \ 8\% \leq SM_{HPC} \leq 20\%\}
\end{aligned}$$

$$\begin{aligned}
U = \{&-800\ ft\text{-}lbf \leq M_{LPS,H} \leq 0\ ft\text{-}lbf \\
&-500\ ft\text{-}lbf \leq M_{HPS,H} \leq 0\ ft\text{-}lbf\}
\end{aligned}$$

where the thrust is omitted from the output constraint set. The input constraints limit EM operation to power extraction only for the healthier engine. The constraint sets are based on standard operating limits for the AGTF30 system but modified to be more conservative and highlight the effectiveness of the

MPC when faced with constraint bounds. To emphasize constraint adherence, $T_{45,\,max}$ is a user-defined temperature constraint applied during simulations. While the remaining constraints are always applied, for the purposes of analysis when $T_{45,\,max}$ is adjusted from its default maximum value of 2414 °R, the HEALED MPC is considered constrained, and when it is equivalent to that value, it is considered unconstrained. At the 50% degradation case, $T_{45,\,max}$= 2205 °R, and at the 100% degradation case, $T_{45,\,max}$ = 2225 °R.

TABLE I. THRUST BALANCING RESULTS

| | *Degraded Engine Condition (%)* | *Total Net Thrust (lbf)* | *Net Thrust Difference (lbf)* | *% of Total Net Thrust* |
|---|---|---|---|---|
| Baseline | 0 | 11488 | 0 | 0 |
| | 50 | 11488 | 23 | 0.20 |
| | 100 | 11488 | 61 | 0.53 |
| HEALED MPC (Unconstrained) | 0 | 11488 | 0 | 0 |
| | 50 | 11488 | 1 | 0.01 |
| | 100 | 11488 | 0 | 0 |
| HEALED MPC (Constrained) | 0 | 11488 | 0 | 0 |
| | 50 | 11488 | 0 | 0 |
| | 100 | 11488 | 0.08 | 0 |

To confirm that HEALED MPC balances thrust, a subsection of the initial test from [9] is repeated. These results are displayed in Table I, which presents thrust balancing results for the Baseline Control and the HEALED MPC. HEALED MPC can balance the thrust asymmetry within 1 lbf, which is significantly less than the Baseline Control.

HEALED MPC balances thrust, but the studied configuration does not reduce the fuel burned as a result. The Baseline Control burns a total of 5469 pounds of fuel per hour in simulation with 100% degradation on the more degraded engine. HEALED PI burns 5467 pounds per hour. And the constrained HEALED MPC matches the baseline with 5469 pounds of fuel burned per hour.

TABLE II. ADHERENCE TO SYSTEM CONTRAINTS ON $T_{45}$

| | *Degraded Engine Condition (%)* | *$T_{45}$ (°R)* | |
|---|---|---|---|
| | | *Degraded Eng.* | *Healthy Eng.* |
| Baseline | 0 | 2191 | 2191 |
| | 50 | 2244 | 2190 |
| | 100 | 2321 | 2187 |
| HEALED MPC (Unconstrained) | 0 | 2191 | 2191 |
| | 50 | 2223 | 2211 |
| | 100 | 2279 | 2229 |
| HEALED MPC (Constrained) | 0 | 2191 | 2191 |
| | 50 | 2231 | 2203 |
| | 100 | 2287 | 2221 |

Table II displays the MPC's ability to follow a system constraint on the healthier engine's $T_{45}$. The healthier engine using HEALED PI reaches 2205 °R and 2228 °R at 50% and 100% degradation scenarios, respectively. Using unconstrained HEALED MPC, the healthy engine reaches 2211 °R and 2229 °R. When temperature constraints are enforced, the HEALED MPC keeps the healthy engine within the prescribed limits.

HEALED MPC penalizes LPC and HPC stall margin (SM) reduction on the healthier, right engine during both constrained and unconstrained control, represented earlier by the output constraint set *Y*. Fig. 5 displays the resulting LPC SM approximations for the Baseline Control, HEALED PI, and HEALED MPC. Stall margin is approximated here based on the modeled compressor maps within the AGTF30 [11]. These results point to the degree of sacrificial stall margin reduction on the healthier engine. The constrained HEALED MPC commands power transfer primarily on the LPS which results in an increased healthier engine LPC SM when compared to the other controllers. The MPC increases LPC SM as intended, but the result is greater than the Baseline case. The intention of HEALED MPC is to preserve healthier engine performance by adhering to system constraints while balancing asymmetric thrust using power transfer. The results show successful adherence to the chosen HEALED MPC constraint set, though in future work, MPC constraint bounds on the healthier engine SM should be chosen such that the upper bound prevents unnecessary SM increase.

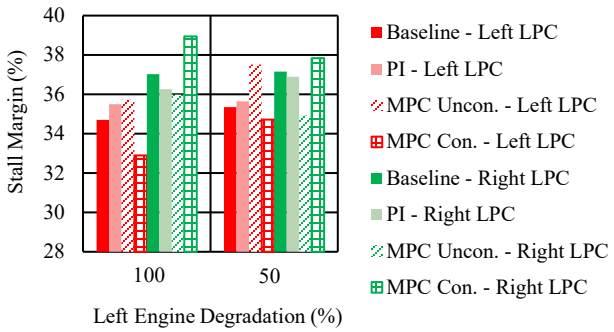


Fig. 5. HEALED LPC Stall Margin

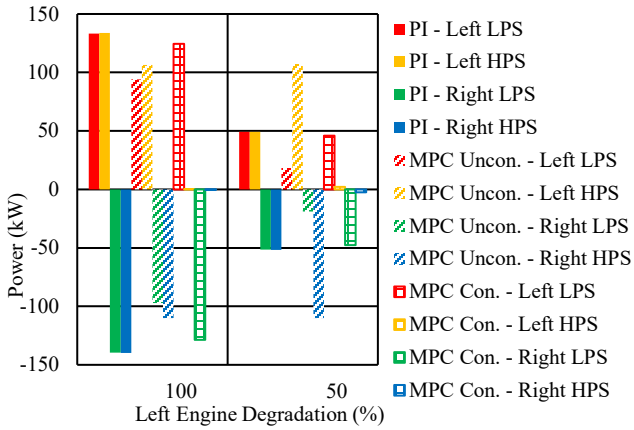


Fig. 6. HEALED EM Power at Cruise.

To achieve balanced thrust, HEALED utilizes the aircraft hybrid-electric power system to transfer extracted power from

the healthier engine to the more-degraded engine. Fig. 6 shows the comparison between HEALED PI and HEALED MPC electrical power results, which highlights that HEALED MPC utilizes the EMs differently than HEALED PI. Whereas HEALED PI maintains an even distribution of power extraction among the EMs, HEALED MPC presents uneven distributions of power extraction which vary in intensity given the unconstrained or constrained condition. The unconstrained HEALED MPC uses both LPS and HPS EMs, maintaining consistently distributed HPS EM use across degradation levels while gradually increasing the contribution from the LPS EM across degradation levels. The constrained HEALED MPC uses the HPS EMs much less and increases the contribution from the LPS EMs as engine degradation increases. These results follow the inability to share power between LPS and HPS EMs. The LPS EMs are assumed to be connected on a common bus isolated from another common bus connecting the HPS EMs.

## VI. Conclusions

This paper presents the HEALED control strategy implemented with MPC, termed HEALED MPC. The controller successfully balances asymmetric thrust on a simulated twin-engine aircraft at steady-state cruise conditions while adhering to system constraints. The chosen constraint set is applied to the healthier engine to preserve performance while power is extracted and inserted onto the more degraded engine utilizing a hybrid-electric powertrain. MPC output constraints on healthier engine turbine temperature and compressor stall margins are applied. In the absence of the temperature constraint, the proposed control architecture used a combination of both LPS and HPS EMs to balance thrust, with an emphasis on using the HPS EM for power extraction. However, this trend reversed in the presence of the temperature constraint where little to no HPS EM torque was commanded, and LPS EM torque was utilized for power extraction. Future research could explore a modification to the electrical power system design where all EMs are connected to a common DC bus allowing power to be more freely distributed between shafts. This would require a re-linearization of the full-system model to include the EPS in the MPC algorithm. Modifications to the powertrain design and improved MPC output constraints could lead to engine performance benefits and the identification of an optimal power extraction ratio between shafts at any given operating point. Finally, since this specific configuration of HEALED MPC failed to reduce fuel burn while balancing the asymmetric thrust, an improved solution is still needed. In future work, additional output constraints should be added to the set with the goal of reducing fuel burn in addition to balancing thrust and adhering to system limits.

## Acknowledgment

The authors would like to acknowledge the Electrified Powertrain Flight Demonstration and Advanced Air Transport Technology projects for funding this work. Thank you to Dr. Joseph Connolly and Donald Simon for your continued help in developing this concept.

## References

[1] Federal Aviation Administration, "United States 2021 Aviation Climate Action Plan," Federal Aviation Administration, 2021.

[2] V. Schultz, H. Schlickenmaier, L. Daelemans, C. Genster, M. Walz, E. Holtz and E. Lovelace, "A Call to Action to Engage the Community to Meet the Challenges that Must be Tackled to Make Electrified Aircraft Propulsion Real," in *34th Congress of the International Council of the Aeronautical Sciences*, Flourence, Italy , 2024.

[3] J. Kratz, J. Connolly, A. Amthor, H. Buescher, S. Bianco and D. Culley, "Turbine Electrified Energy Management for Single Aisle Aircraft," in *IEEE/AIAA Electrified Aircraft Technologies Symposium*, Anaheim, California, 2022.

[4] J. Chapman, "A Study of Large Scale Power Extraction and Insertion on Turbofan Performance and Stability," in *AIAA/IEEE Electric Aircraft Technologies Symposium*, New Orleans, Louisiana, 2020.

[5] T. Chau and R. Jansen, "Conceptual Design of the Hybrid-Electric Subsonic Single Aft Engine (SUSAN) Electrofan Transport Aircraft," in *AIAA SciTech Forum* , Orlando, Florida, 2023.

[6] D. C. a. G. T. Jonathan Kratz, "A Control Strategy for Turbine Electrified Energy Management," in *AIAA Propulsion and Energy Forum*, Indianapolis, IN, 2019.

[7] J. Sachs-Wetstone, S. Bianco, J. Kratz, M. Horning, A. Amthor, J. Connolly and J. Saus, "Hybrid-Electric Aero-Propulsion Controls Testbed Results," in *Aviation/Electric Aircraft Technologies Symposium*, San Diego, California, 2022.

[8] J. Chapman and J. Litt, "Control Design for an Advanced Geared Turbofan Engine," in *AIAA Joint Propulsion Conference*, Atlanta, Georgia, 2017.

[9] H. E. Buescher, "Hybrid Electric Aircraft with Unlike Engine Degradation," in *ASME Turbomachinery Conference and Exposition*, London, 2024.

[10] E. Hill, A. E. Amthor, D. I. Soloway, D. L. Simon and J. W. Connolly, "Model Predictive Control Strategies for Turbine Electrified Energy Management," *Journal of Engineering for Gas Turbines and Power,* pp. 1-24, 2023.

[11] J. Kratz, "The Advanced Geared Turbofan 30,000 lbf - electrified (AGTF30-e): A Virtual Testbed for Electrified Aircraft Propulsion Research," in *AIAA/IEEE Electric Aircraft Technologies Symposium*, Las Vegas, Nevada, 2024.

[12] T. Kennings and D. Simon, "MEX Solver and Linearization Tool Users Guide V1.4," 13 January 2025. [Online]. Available: https://github.com/nasa/-AGTF30-mex-solver-/blob/main/documentation/MEX%20Solver%20and%20Linearization%20Tool%20Users%20Guide%20V1.4.pdf. [Accessed 4 February 2025].

[13] J. Litt, T. S. Sowers and S. Garg, "A Retro-Fit Control Architecture to Maintain Engine Performance with Usage," in *18th ISABE Conference*, Beijing, China, 2007.

[14] J. B. Rawlings and D. Q. Mayne, Model Predictive Control: Theory and Design, 2nd ed., Madison: Nob Hill Publishing, 2009.

[15] P. Kumar, Y. K. Al-Nadawi and M. Ilak, "Fast real-time power splitting for hybrid electric propulsion using neural network based approximate model predictive control," in *AIAA SciTech 2024 Forum*, Orlando, 2024.

[16] M. Doff-Sotta, M. Cannon and M. Bacic, "Data-Driven Robust Model Predictive Control of Tiltwing Vertical Takeoff and Landing Aircraft," *Journal of Guidance, Control, and Dynamics,* vol. 0, no. 0, pp. 1-9, 2024.

[17] Z. Jiang and S. A. Raziei, "Hierarchical Model Predictive Control for Real-Time Energy-Optimized Operation of Aerospace Systems," in *2019 AIAA/IEEE Electric Aircraft Technologies Symposium (EATS)*, Indianapolis, 2019.

[18] S. Qu, T. He and W. Su, "Mixed Model Predictive Control and Data-Driven Control of a Tiltrotor eVTOL Aircraft," in *AIAA SciTech Forum*, Orlando, 2024.